Elastic behavior associated with phase transitions in incommensurate Ba$_2$NaNb$_5$O$_{15}$

J. Herrero-Albillos,[1] P. Marchment,[2] E. K. H. Salje,[2] M. A. Carpenter,[2] and J. F. Scott[2]

[1]*Department of Materials Science, University of Cambridge, Pembroke Street, Cambridge CB2 3QZ, United Kingdom*
[2]*Department of Earth Sciences, University of Cambridge, Downing Street, Cambridge CB2 3EQ, United Kingdom*

The elastic behavior of barium sodium niobate (Ba$_2$NaNb$_5$O$_{15}$) has been investigated by resonant ultrasound spectroscopy through six different structural phases, with emphasis on the five incommensurate phase transitions near 40, 110, 547, 565, and 582 K. Data near 40 K are at least consistent with the existence of a lock-in transition to *P4nm* at that temperature [Filipic *et al.*, J. Phys.: Condens. Matter **19**, 236206 (2007)], which has been controversial. A relaxation process occurs around the transition near 110 K and is assigned to a process involving movement of domain walls of the phase. Unusual behavior is observed through the high-temperature incommensurate transitions with large variations in frequency in the ultrasonic resonances, and a broad peak in the dissipation. No clear signature of the 1q-2q incommensurate-incommensurate transition at 565 K is observed. This is compatible with a model in which incommensurate-incommensurate transitions are not expected to manifest elastic anomalies.

PACS number(s): 64.70.Rh, 62.20.dq, 77.84.−s

I. INTRODUCTION

Barium sodium niobate, Ba$_2$NaNb$_5$O$_{15}$ (BNN), is a ferroelectric material that undergoes six phase transitions, with three incommensurate phases and a rare phase transition between two incommensurate phases. The incommensurate modulations are along directions perpendicular to the ferroelectric polarization and unusually for an incommensurate ferroelectric, BNN keeps its remanent polarization to very low temperatures.[1] BNN also displays useful optical and electro-optic properties, being useful as a frequency doubling material and having good resistance to optical damage.[2] BNN is also used, such as LiNbO$_3$ and KTiOPO$_4$, as a periodically poled nonlinear optical device material.[3] The behavior of BNN is further complicated as a result of most samples being nonstoichiometric with a large variability in the concentration of Na vacancies, sometimes as high as 10%.[4]

BNN has the tetragonal tungsten bronze structure at high temperatures[2] and undergoes a ferroelectric transition near 830 K. The phase diagram of BNN is shown in Fig. 1. The system is incommensurate between 582 and 547 K, with a transition from a high temperature 2q phase to a 1q phase within this region, near 565 K. There are two phase transitions below room temperature, near 110 K, from the quasicommensurate room temperature phase to a 2q tetragonal phase, followed by a "lock-in" transition near 40 K.[5,6] The incommensurate modulations occur in the plane perpendicular to the ferroelectric polarization and this material remains ferroelectric to high temperatures.[2,7]

The ferroelectric transition involves a loss of the mirror plane perpendicular to the c axis, with no change in the unit cell orientation. The transition is slightly first order, but is strongly affected by the stoichiometry of the sample, with samples containing higher concentrations of Na vacancies exhibiting a ferroelectric transition with tricritical dynamics and a shift in the apparent Curie temperature.[8] The high-temperature 2q incommensurate phase consists of two orthogonal modulations, one of which is long range and the other short range.[9] It undergoes a transition to a 1q incom-

mensurate phase, losing the short range modulations. The 2q phase is explained by Scott *et al.*[8] as a wall roughening of the 1q phase, with the 1q-2q phase transition resulting in a change of the effective point group from tetragonal (2q) to orthorhombic (1q). The two incommensurate phases may coexist, and a complicated memory effect in the incommensurate region has been observed.[10] The "quasicommensurate" orthorhombic phase retains a residual incommensurability below the transition near 547 K[10,11] due to pinning by defects (Na vacancies).

The 2q phase present from 110 to 40 K has an effective point group which is tetragonal, but despite the similarities to the 2q phase at high temperatures, it is not re-entrant.[12] The lock-in transition near 40 K was predicted by Schneck[4] and first detected by Scott *et al.*,[13] although more recent studies have failed to detect it.[14,15] The difficulty in observing the transition arises because of the likelihood that Na vacancies stabilize the incommensurate phase and the kinetic limitations of the transition.[12]

Most previous studies of the elastic behavior of BNN have been obtained by Brillouin spectroscopy, or performed at low frequency using torsion pendulum methods. A torsion
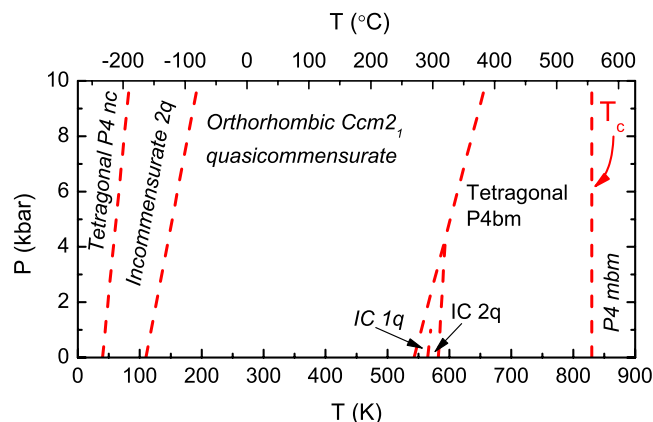
FIG. 1. (Color online) Schematic phase diagram of barium sodium niobate after Refs. 9, 23–25, 32, and 34.

pendulum study[16] and a study[7] involving measurement of resonant vibrations in bars and plates of BNN showed anomalies in the elastic constants, and showed peaks in dissipation associated with the high-temperature incommensurate transitions.[16] A Brillouin scattering study[17] showed anomalies in the elastic constants C_{11} and C_{22} at the transition near 110 K. A series of torsion pendulum studies,[18–20] investigated shear modulus and dissipation in BNN, observing anomalies in the shear modulus and peaks in dissipation associated with the transitions near 830, 110 K, and the high-temperature incommensurate region. A large relaxation peak at 228 K was also observed.

In the present study the elastic properties of BNN are investigated using resonant ultrasound spectroscopy (RUS). The general method of carrying out the experiments is to balance the sample, in the form of a parallelepiped, on its opposite corners between two piezoelectric crystals, one of which is used to drive the oscillations, and the other to detect the response of the sample. The vibrational modes of a parallelepiped (typically in the frequency range of ~ 0.1–2 MHz) can be calculated[21] and when the sample shape, mass, and space group are known, a computational analysis of the resonant frequencies allows the resonances to be assigned to specific combinations of elastic constants.[22] The dissipation associated with the vibrations can be obtained from the shape of the resonance peaks. RUS offers a number of advantages over other methods of measuring elastic constants, being able to determine all of the elastic constants from a single spectrum, giving a higher accuracy when comparing elastic constants. It is also possible to use small samples, down to ~ 1 mm. Irregular shaped samples can be used, although the determination of elastic constants may not then be possible.[21]

This study aims to follow the elastic constants and mechanical quality factor of ultrasonic resonances in BNN through all the phase transitions. The observed variations will be discussed in terms of the insights they provide into the nature of the transitions. Other processes unrelated to the phase transitions may also be detected by changes in the elastic constants and attenuation.

II. EXPERIMENTAL DETAILS

The $Ba_2NaNb_5O_{15}$ sample used was a single crystal with $\sim 0.5\%$ Na vacancies used in previous studies of the dielectric and heat capacity behavior of BNN.[8,12] The crystal had mass 0.08 g, and an irregular shape which can be approximated as a parallelepiped with dimensions $3.9 \times 2.1 \times 2.1$ mm^3 (the two square faces are miss aligned by up to a 12%, while a 3% deviation is observed between the other faces). The long axis was parallel to the tetragonal c axis. Because this sample had been used in previous studies and to allow direct comparison with other data collected from it, we elected not to recut it: RUS spectra were recorded in the range of 10–920 K. Low-temperature spectra were recorded at intervals of 30 K during cooling and 5 K during heating, with at least 15 min between each scan for thermal equilibration. High-temperature spectra were recorded at intervals of 10 and 5 K in the vicinity of phase transitions, during

heating and cooling, with 5 min between each scan. A second run was performed in the proximity of the high-temperature incommensurate phase, collecting spectra every 2 K, during both cooling and heating. A second 0.02 g crystal, with an irregular shape measuring approximately 3–4 mm across, known to have a 3% Na-vacancy concentration,[12] was also studied in the 300 to 650 K temperature range. Spectra were collected in the frequency range 400–1200 kHz (100–1100 kHz for the second sample) and each contained 50 000 data points. The RUS equipment for low and high temperatures used in this work has been previously described in detail by McKnight *et al.*[26,27] The crystals were mounted across a pair of corners in each case, not using any bond. Analysis of the spectra was carried out using the software package Igor Pro (wavemetrics). Peaks for selected resonances were fitted using an asymmetric Lorentzian function also used in Refs. [26] and [27] to obtain their frequencies, f, and widths at half maximum height, Δf. An analogous approach is described in Refs. [28] and [29]. The inverse mechanical quality factor, Q^{-1}, was calculated as $Q^{-1} = \Delta f / f$.

It was not possible to extract individual elastic constants from the frequencies directly because the alignment and shape of the crystal was too far removed from the ideal geometry of a parallelepiped. Nevertheless, likely dependences of the resonance modes on specific elastic constants were suggested by two factors. First, use of the software described by Migliori and Sarrao[30] for a parallelepiped with the dimensions given above, faces aligned parallel to (100), (010), and (001), and single crystal elastic constant values given by Denda and Mansukh,[31] indicated that the low-frequency resonances are dominated primarily by the influence of C_{33}, C_{44}, or combinations of the two. Second, the form of elastic softening at the ferroelectric transition is expected to be dependent on coupling of strains, e_i, with the order parameter, Q, as $\lambda e_3 Q^2$ and $\lambda e_4^2 Q^2$, which would give a step like function for C_{33} and a relatively smooth variation of C_{44}.[32,33] As discussed below, distinctive patterns of frequency variations for some of the observed resonances through the transition near 830 K are consistent with these assignments.

III. RESULTS AND DISCUSSION

Figure 2 shows the measured RUS spectra for BNN from 10 to 930 K, with a vertical offset proportional to the temperature. Upon heating from low temperatures all the peaks show a decrease in frequency until the resonances reach their minimum frequencies near 500 K. The frequency of the resonances then increases through the high-temperature incommensurate region to reach their maximum values in the region of 650–750 K. They all show a pronounced reduction in frequency just below the ferroelectric transition near 830 K before rising sharply above this temperature. The main differences in the frequency behavior of the resonances occur in the relative effects at the different transitions. In general the resonances show dissipation associated with all of the phase transitions, particularly through the incommensurate region between 582 and 547 K. Additional broad peaks in the frequency region of 850–1050 kHz of the low temperature spectra are instrumental in origin.
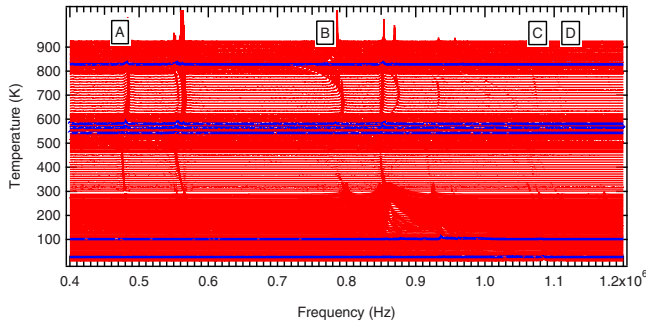
FIG. 2. (Color online) RUS spectra for single crystal BNN for frequencies in the region 400–1200 kHz. Above room temperature, spectra were recorded at intervals during cooling from 920 K to room temperature from the first data collection. Below room temperature, spectra were recorded at intervals during heating from 10 K to room temperature. The *y* axis is amplitude, with spectra displaced in proportion to their temperature. The amplitude of the low temperature spectra has been scaled down by a factor of 0.05 for ease of comparison. Spectra collected at temperatures close to the six different structural phases are shown in blue. Labels A, B, C, and D correspond to the resonances described in the text.

Here we report the temperature evolution of the frequency and inverse mechanical quality factor (Q^{-1}) for selected resonances: namely, resonances A and B for the whole temperature range (475–488 kHz and 720–840 kHz, respectively), resonance C for the low-temperature region (1068–1085 kHz) and resonance D to study the high temperature incommensurate transition (1110–1124 kHz). Based on the considerations given in Sec. II, resonance A is presumed to be dominated by the influence of C_{44}, while resonances B and C are dominated by the influence of C_{33}. Resonance D depends on both. The high temperature incommensurate transition was further studied using the second sample; the temperature evolution of the frequency for resonances E and F are presented here (319–321 kHz and 872–884 kHz, respectively). Note that the positions of the latter resonances do not correspond to those in the first sample, since the specimens had different shapes and masses.

A. Low-temperature phase transitions

Figure 3 shows the evolution of the frequency and Q^{-1} for resonances A–C from 10 K to room temperature. At the lowest temperatures Q^{-1} has a smooth increase with temperature, departing from a linear behavior above 50 K, to reach a rounded maximum at 160 K. A smaller maximum in the dissipation can also be observed at 250 K. Those two maxima at 160 and 250 K in Q^{-1} are related respectively to the R1 and R2 relaxation processes recently reported in BNN from dielectric measurements.[12] The frequency of the three resonances essentially decreases with increasing temperature, with changes of slope near 70, 180, and 235 K.

All resonances show a leveling off with falling temperature characteristic of standard third law thermodynamics. In this case, however, the obvious change in trend of Q^{-1} coincides with the low temperature lock-in phase transition near 40 K predicted by Schneck[4] and first detected by Scott *et*
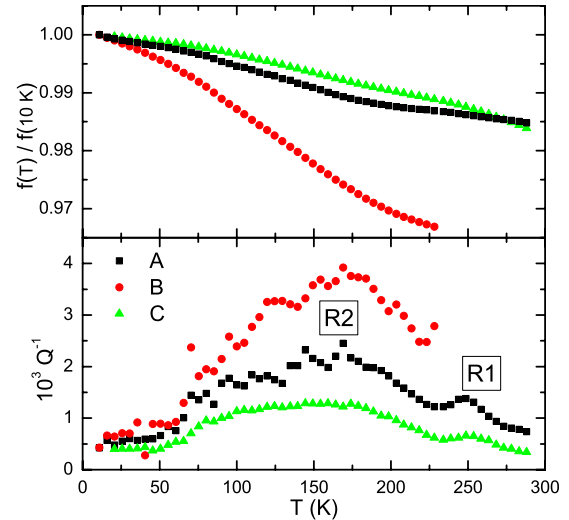
FIG. 3. (Color online) Low temperature variation in the frequency (top) and Q^{-1} (bottom) with temperature for resonances A (black squares), B (red circles), and C (green triangles). The frequency for each resonance has been divided by the value at 10 K for a better comparison.

al.[13] This transition was not found in some later studies[14,15] but was recently shown to be unambiguously present and limited by kinetics in our sample.[12] We suggest that the transition is marked, in particular, by a change in acoustic dissipation behavior.

The R2 relaxation is associated with the transition from the room-temperature quasicommensurate phase to the low temperature $2q$ incommensurate phase. Although it is identified as the R2 resonance, it is spread over a wider temperature interval (80–230 K) than the observed anomaly near 130 K by Gridnev *et al.*[18,20] at low frequencies; it is observed in a similar range to the one over which elongation of microdomains along [010] was found to occur in Ref. 14. This is probably due to the process described in Ref. 20 as a fluctuational nucleation of a phase and motion of interphase boundaries through a system of obstacles. The existence of a two-phase region down to 85 K is suggested in Ref. 34.

A relaxation peak at 228 K was reported in Ref. 18, where it was explained as being due to the interaction between immobile domain walls with charged point defects—most likely Na vacancies—which can diffuse to counteract the piezoelectric polarization induced in the domains by an applied stress. The peak in Q^{-1} is caused by the anelastic deformation of the crystal that accompanies this diffusion. This might be the same process as observed at 250 K (R1) in the present study, with the difference in temperature of the peaks accounted for by the higher frequency at which the RUS experiment was carried out.

B. High-temperature incommensurate phases

The upper panel of Fig. 4 shows the variation in frequency for resonances A and D from room temperature to temperatures above the high-temperature incommensurate phases. The two curves for resonance A correspond to the first and second run; the small mismatch below the $1q$-$2q$
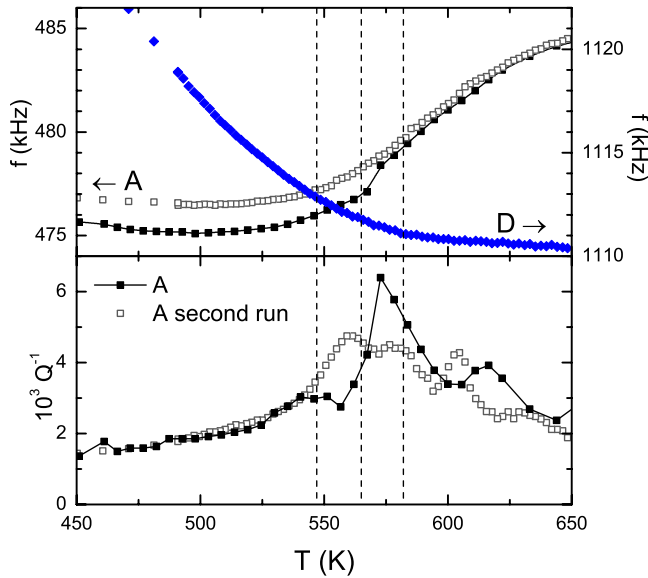
FIG. 4. (Color online) Variation in frequency (top) and Q^{-1} (bottom) with temperature in the vicinity of the high temperature incommensurate transition, for resonances A (black squares), D (blue diamonds), as well as the values for resonance A obtained from a second measurement (open squares).

transition at 565 K is most likely due to slight variations in microstructure arising at this transition during different heating/cooling cycles. The data for resonance D were obtained from spectra in the second run, in which the resonance was more strongly excited.

It is clear from Fig. 4 that the frequencies of resonances A and D have very different evolution with temperature through the 547, 565, and 582 K transitions. It is interesting to note that neither shows any abrupt anomaly at those temperatures. Because we are dealing with linear elasticity here we can invoke a model that is not generally true for nonlinear elasticity. In this linear case only the macroscopic symmetry change matters at $k=0$. Any symmetry-breaking transition is prone to anomalies in the elastic constants. For ferroelastic materials we have the symmetry breaking at $k=0$. Commensurate-incommensurate transitions also break symmetry because here we have a $k=0$ anomaly superposed onto a modulation at another k vector which is not in resonance (and does not add up to a $k=0$ wave, as would occur for a zone-boundary antiferrodistortive transition as, for example in $SrTiO_3$ near 105 K). Only the $k=0$ part matters, the rest of the Brillouin zone does not. Changes between $1q$ and $2q$ phases would not show any elastic anomalies as long as the $k=0$ symmetry is the same. Strong nonlinearities can occur for simple geometrical reasons while strong nonlinear coupling between modulations with orthogonal wave vectors are usually very weak. Power law singularities near interfaces[35] would only lead to signals proportional to the volume proportion of the interfaces.[36] Even extreme nonlinear coupling with secondary degrees of freedom[37] do not result in strong elastic anomalies.

Accompanying the softening of resonance A associated with the temperature interval of IC transitions is a broad increase in dissipation (see Fig. 4). Additional details in the
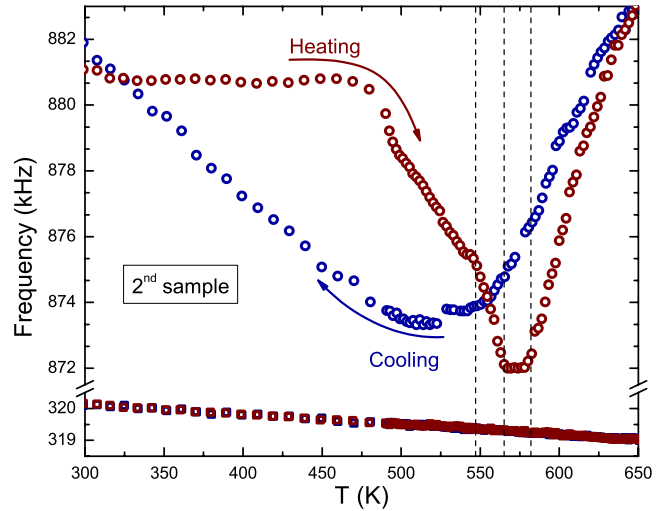
FIG. 5. (Color online) Variation in frequency with temperature in the vicinity of the high-temperature incommensurate transition, for resonances E (open squares), F (open circles) in a second BNN sample for both the heating and cooling runs.

variations of Q^{-1} evident in the data are not reliable due to the influence of baseline noise on resonance peaks which are already weak and broad, but the overall pattern is clear. The observed behavior is unusual, however, in that a normal relaxation process would be expected to display elastic stiffening below and softening above the temperature at which the dissipation reaches a maximum. It may be related to the memory effect observed in Refs. 10 and 38 a behavior which was also observed in the study of shear strains in BNN by Biryukov *et al.*[16] The peak in Q^{-1} was explained in Ref. 20 by domain-wall dynamics and structure. There is also a central peak mode observed by Raman spectroscopy by Scott *et al.*,[13] which has essentially the same temperature dependence as shown in Fig. 4.

Although no significant hysteresis was observed for the first sample, some of the resonances found in the second sample displayed a very pronounced thermal hysteresis across the incommensurate phase transitions. The temperature dependence of the frequency of resonances E and F has been plotted in Fig. 5 for both heating and cooling runs. The patterns of variations shown by these closely resemble the pattern of variations of Brillouin peaks which depend largely on C_{11}/C_{22} and C_{44}, respectively, as observed by Errandonea *et al.*[32] The second sample also contains a higher concentration of Na vacancies than the first, and the results are consistent with the conclusion of Ref. 32 that there are strong interactions between the incommensurate modulations and defects which have a significant impact on the elastic properties. The frequency of resonance F for the heating run also shows a more abrupt change with temperature than for the cooling run, in good agreement with the different evolution when cooling/heating of the misfit parameter through the $1q$-$2q$ transition; see Kiat *et al.*[38] The origin of both the thermal hysteresis and the different abruptness of the transition when cooling/heating lies in the difficulty of phase $1q$ to nucleate into the $2q$ phase, leading to a continuous transition upon cooling.
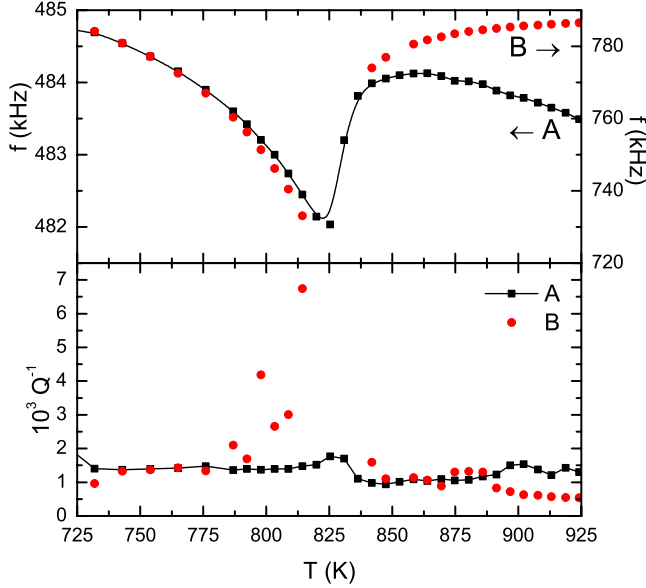
FIG. 6. (Color online) Variation in frequency (top) and Q^{-1} (bottom) with temperature in the vicinity of the ferroelectric transition, for resonances A (black squares) and B (red circles).

C. Ferroelectric phase transition

Figure 6 shows the temperature dependence of the frequency and Q^{-1} for the resonances A and B in the proximity of the ferroelectric transition. Both resonances show an anomaly near 825 ± 5 K, with a clear minimum in the frequency and maximum in the dissipation. However, the change in frequency is 20 times larger for resonance B (note the different scales in the y axes in upper panel of Fig. 6). This pattern of evolution can be understood in terms of the mean field behavior described by a Landau expansion for the $P4/mbm \rightarrow P4bm$ transition,

$$G = \frac{1}{2}a(T - T_c)Q^2 + \frac{1}{4}bQ^4 + \frac{1}{6}cQ^6 + \lambda_1(e_1 + e_2)Q^2 + \lambda_3 e_3 Q^2$$

$$+ \lambda_4(e_4^2 + e_5^2)Q^2 + \lambda_5(e_1 - e_2)^2 Q^2 + \lambda_6 e_6^2 Q^2$$

$$+ \frac{1}{4}(C_{11}^o + C_{12}^o)(e_1 + e_2)^2 + \frac{1}{4}(C_{11}^o - C_{12}^o)(e_1 - e_2)^2$$

$$+ C_{13}^o(e_1 + e_2)e_3 + \frac{1}{2}C_{33}^o e_3^2 + \frac{1}{2}C_{44}^o(e_4^2 + e_5^2) + \frac{1}{2}C_{66}^o e_6^2,$$

where Q here is the order parameter, a, b, and c are the Landau coefficients, λ_1 to λ_6 are the strain/order parameters coupling coefficients, e_1 to e_6 are the strains, and C_{ik}^o are the elastic constants of the parent $P4/mbm$ structure. On this basis, and following Slonczewski and Thomas,[39] the elastic constants C_{44} and C_{33} would be expected to behave as

$$C_{33} = C_{33}^o - 4\lambda_3^2 Q^2 \left(\frac{\partial^2 G}{\partial Q^2}\right)^{-1},$$

$$C_{44} = C_{44}^o + 2\lambda_4 Q^2.$$

At a second order transition, C_{33} would show a simple step, with the amount of softening below T_c depending on the
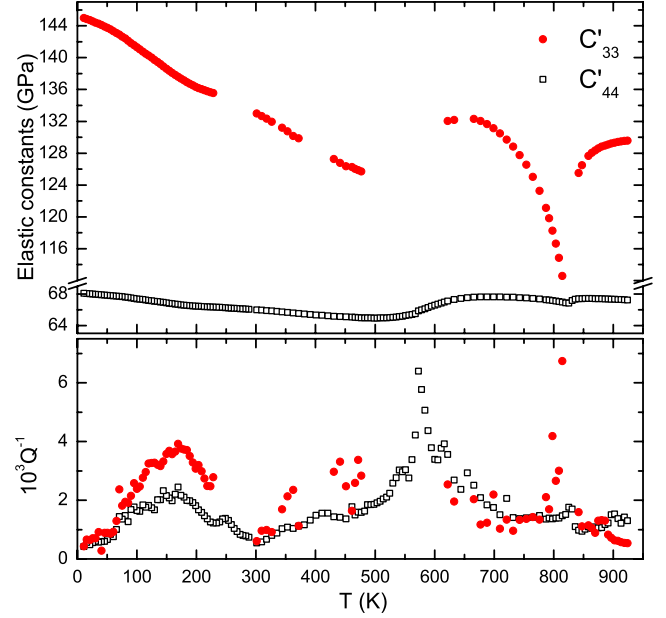
FIG. 7. (Color online) Overview of the elastic constant and dissipation behavior of BNN from the present study. Values of C_{33} and C_{44} have been estimated on the basis of room temperature elastic constant data of Denda and Mansukh (Ref. 31) and assumed assignments of resonances A and B. They have been labeled as C'_{33} and C'_{44} to signify that their variations are estimated from resonances which do not depend exclusively on C_{33} and C_{44}, respectively.

magnitude of λ_3^2. C_{44} should show a slight softening (or stiffening) which increases linearly with falling temperature. Scott *et al.*[8] showed, however, that the transition is close to tricritical in character $[Q^4 \propto (T_c - T)]$, in which case C_{33} would show additional nonlinear softening as the transition is approached from below (see Ref. 33, for example). The softening or stiffening of C_{44} would still scale with Q^2, and thus be a nonlinear function of temperature. The observed variation of resonance B is consistent with being determined by C_{33} and tricritical behavior. The small frequency step in resonance A can be explained if it is due to a small component of C_{33} controlling this distortional mode which is otherwise determined by C_{44}. Variations in the actual values of C_{33} and C_{44} throughout the entire temperature range for which data were collected have then been estimated by taking $C_{33} = 133$ GPa and $C_{44} = 66$ GPa as room-temperature values from Denda and Mansukh,[31] and scaling the frequencies of resonances A and B as if they are dependent on C_{33} and C_{44} as $C'_{33} = 2.09 \times 10^{-10} f_B^2$ and $C'_{44} = 2.88 \times 10^{-10} f_A^2$ (see Fig. 7). The prime has been added here and in Fig. 7 to emphasize that the resonance frequencies do not depend exclusively on C_{33} and C_{44}

The anomaly in the frequency at the ferroelectric transition is accompanied by a peak in Q^{-1} for resonance A and a peak (or possible discontinuity) in Q^{-1} for resonance B. This anomaly in Q^{-1} has been also reported in Refs. 19 and 20. Since both the paraelectric and ferroelectric phases are tetragonal[2] the anomaly cannot originate from ferroelastic twinning.

IV. CONCLUSIONS

Phase transitions in BNN give rise to significant changes in elastic properties when probed by RUS at 0.1–1.2 MHz. The $P4/mbm \leftrightarrow P4bm$ transition shows elastic anomalies which are consistent with mean-field tricritical behavior. The high-temperature incommensurate phase transitions occur in a temperature interval which is marked by significant elastic softening, though changes in the elastic constants are continuous. Assignment of C_{33} to one of the resonance would imply that there could be coupling between the ferroelectric and incommensurate order parameters via the common strain e_3. The two low-temperature transitions do not give rise to discrete changes in the elastic constants which determine the observed resonances, suggesting that they involve a relatively subtle change in structure with minimal strain relaxation or that they are smeared over some relatively wide temperature interval. The final transition occurs close to where the temperature dependence of the elastic constants starts to tend toward zero.

Data for acoustic dissipation provide different, though incompletely understood insights into the relaxational processes which take place in BNN. The ferroelectric transition gives a classical increase in dissipation just below T_c which would normally be associated with twin wall motion in a ferroelastic material. By symmetry, however, there are no ferroelastic twin walls and the dissipation may be intrinsic. The incommensurate phases are accompanied by significant increases in dissipation which appear to be at least partly dependent on defects. In principle, the dissipation behavior should contain information on interactions between antiphase boundaries and defects. In the low-temperature region, a broad anomaly appears to be related to the development of microdomains inferred from other measurements. The lowest temperature transition, near ~40 K, seems to involve only an increase in dissipation behavior with increasing temperature.

Determination of lattice parameters to high resolution would certainly help to resolve the question of which of these relaxational phenomena are associated with conventional strain/order parameter coupling at discrete phase transitions and which are due to additional dynamic effects.

[1] S. Mori, N. Yamamoto, Y. Koyama, S. Hamazaki, and M. Takashige, Phys. Rev. B **52**, 9117 (1995).

[2] K. S. Rao and K. H. Yoon, J. Mater. Sci. **38**, 391 (2003).

[3] A. Rodenas, D. Jaque, F. Agullo-Rueda, and A. A. Kaminskii, Opt. Commun. **262**, 220 (2006).

[4] J. Schneck, Ph. D. thesis, University of Paris VI, 1982.

[5] J. Schneck, D. Primot, R. Von der Muhll, and J. Raves, Solid State Commun. **21**, 57 (1977).

[6] W. F. Oliver and J. F. Scott, Ferroelectrics **117**, 63 (1991).

[7] T. Yamada, H. Iwasaki, and N. Niizeki, J. Appl. Phys. **41**, 4141 (1970).

[8] J. F. Scott, S. A. Hayward, and M. Miyake, J. Phys.: Condens. Matter **17**, 5911 (2005).

[9] C. Manolikas, J. Schneck, J. C. Toledano, J. M. Kiat, and G. Calvarin, Phys. Rev. B **35**, 8884 (1987).

[10] J. M. Kiat, G. Calvarin, and J. Schneck, Phys. Rev. B **49**, 776 (1994).

[11] J. C. Toledano, J. Schneck, and G. Errandonea, *Incommensurate Phases in Dielectrics, Modern Problems in Condenses Matter Sciences* (North-Holland, Amsterdam, 1985).

[12] C. Filipic, Z. Kutnjak, R. Lortz, A. Torres-Pardo, M. Dawber, and J. F. Scott, J. Phys.: Condens. Matter **19**, 236206 (2007).

[13] J. F. Scott, A. Shawabkeh, W. F. Oliver, A. C. Larson, and P. Vergamini, Ferroelectrics **104**, 85 (1990).

[14] S. Mori, N. Yamamoto, Y. Koyama, and Y. Uesu, Phys. Rev. B **55**, 11212 (1997).

[15] K. Fujishiro and Y. Uesu, J. Phys.: Condens. Matter **8**, 6435 (1996).

[16] A. V. Biryukov, S. A. Gridnev, O. N. Ivanov, A. V. Vasileva, and L. F. Kirpichnikova, Ferroelectrics **359**, 70 (2007).

[17] M. S. Zhang, T. Yagi, W. F. Oliver, and J. F. Scott, Phys. Rev. B **33**, 1381 (1986).

[18] S. A. Gridnev, A. V. Biryukov, and O. N. Ivanov, Phys. Solid State **43**, 1735 (2001).

[19] S. A. Gridnev, A. V. Biryukov, and O. N. Ivanov, Ferroelectr., Lett. Sect. **25**, 11 (1999).

[20] S. A. Gridnev, A. V. Biryukov, and O. N. Ivanov, Ferroelectrics **219**, 1 (1998).

[21] A. Stekel, J. L. Sarrao, T. M. Bell, L. Ming, R. G. Leisure, W. M. Visscher, and A. Migliori, J. Acoust. Soc. Am. **92**, 663 (1992).

[22] R. G. Leisure and F. A. Willis, J. Phys.: Condens. Matter **9**, 6001 (1997).

[23] T. Kojima, T. Nakamura, K. Asuami, M. Takashige, and S. Minomura, Solid State Commun. **29**, 779 (1979).

[24] T. Kojima, T. Nakamura, K. Asuami, M. Takashige, and S. Minomura, J. Phys. Soc. Jpn. **45**, 1433 (1978).

[25] H. Savary and J. C. Toledano, Phys. Rev. B **31**, 3134 (1985).

[26] R. E. A. McKnight, M. A. Carpenter, T. W. Darling, A. Buckley, and P. A. Taylor, Am. Mineral. **92**, 1665 (2007).

[27] R. E. A. McKnight, T. Moxon, A. Buckley, P. Taylor, T. W. Darling, and M. A. Carpenter, J. Phys.: Condens. Matter **20**, 075229 (2008).

[28] J. Schreuer, C. Thybaut, M. Prestat, J. Stade, and S. Haussuhl, Proc.-IEEE Ultrason. Symp. **2003** 196 (2003).

[29] J. Schreuer and C. Thybaut, Proc.-IEEE Ultrason. Symp. **2005** 695 (2005).

[30] A. Migliori and J. L. Sarrao, *Resonant Ultrasound Spectroscopy: Applications to Physics, Material Measurements and Nondestructive Evaluation* (Wiley, New York, 1997).

[31] M. Denda and M. Mansukh, Eng. Anal. Bound. Elem. **29**, 533

(2005).

[32] G. Errandonea, M. Hebbache, and F. Bonnouvrier, Phys. Rev. B **32**, 1691 (1985).

[33] M. A. Carpenter, E. K. H. Salje, and A. Graeme-Barber, Eur. J. Mineral. **10**, 693 (1998).

[34] A. Shawabkeh and J. F. Scott, Phys. Rev. B **43**, 10999 (1991).

[35] E. K. H. Salje, J. Phys.: Condens. Matter **20**, 485003 (2008).

[36] E. K. H. Salje, Phys. Chem. Miner. **35**, 321 (2008).

[37] L. Goncalves-Ferreira, S. A. T. Redfern, E. Atacho, and E. K. H. Salje, Appl. Phys. Lett. **94**, 081903 (2009).

[38] J. M. Kiat, G. Calvarin, and J. Schneck, Ferroelectrics **105**, 219 (1990).

[39] J. C. Slonczewski and H. Thomas, Phys. Rev. B **1**, 3599 (1970).